Vacuum tunneling spectroscopy and asymmetric density of states of $Bi_2Sr_2CaCu_2O_{8+\delta}$

Ch. Renner and Ø. Fischer
Département de Physique de la Matière Condensée, Université de Genève, 24, Quai E.-Ansermet, CH-1211 Genève 4, Switzerland
(Received 29 November 1994)

This paper reports very detailed low-temperature vacuum tunneling spectroscopy investigations of $Bi_2Sr_2CaCu_2O_{8+\delta}$ (BSCCO) single crystals. For clean vacuum junctions formed between a cleaved BSCCO single crystal and the normal-metal tip of a scanning tunneling microscope, we obtain stable *c*-axis vacuum tunneling conditions that allow very reproducible low-temperature electron tunneling spectroscopy. A vacuum junction is identified by tunneling spectra which neither depend on tip/sample spacing nor change as a function of time and position on the sample in the Meissner state. In contrast to the frequently reported linear or parabolic increase with increasing bias voltage, the background conductance of such spectra is largely constant with a slight decrease up to ±300 meV bias. The normal-state conductance inferred from this background has a local maximum at negative sample bias, indicating a pileup below the Fermi level in the (*ab*)-plane normal-state density of states of BSCCO. Vacuum junctions at 4.8 K show a well developed superconducting gap with large peaks at the gap edges and a finite density of quasiparticle excitations filling the gap. These characteristics are not consistent with an isotropic BCS-like gap parameter. Outside the superconducting gap, the differential conductance curves are very asymmetric, with a striking dip which appears at negative sample bias only. This dip contributes a substantial amount of states to satisfy the conservation of states we find between normal and superconducting BSCCO.

I. INTRODUCTION

The pioneering experiments of Giaever,[1] Fisher and Giaever,[2] and Nicol, Shapiro, and Smith[3] firmly established tunneling spectroscopy as a powerful tool to investigate superconductors. Tunneling provides high-energy-resolution information about the electron density of states (DOS).[4] The superconducting energy gap (Δ) and the electron-phonon coupling of conventional superconductors have been measured with great accuracy using this technique. Excellent agreement was found with theory, demonstrating the validity of the BCS model for conventional superconductors in the weak- and strong-coupling limits.[5] In the case of high-temperature superconductors (HTS's), tunneling spectroscopy is still awaiting agreement among the scientific community. The prevailing controversy is mainly due to the widely scattered experimental data available in the literature.[6] This confusing situation arises from the extreme difficulty in achieving a well controlled tunnel junction on HTS's, a consequence of their short coherence lengths and highly reactive surfaces. However, we believe there are no fundamental reasons why tunneling would fail in revealing the nature of the high-temperature superconducting state, when it proved so successful in understanding conventional superconductors. In this article, we show that relevant tunneling spectroscopy of $Bi_2Sr_2CaCu_2O_{8+\delta}$ (BSCCO) can be obtained in careful scanning tunneling microscope[7] (STM) experiments.

The understanding of the basic mechanism(s) leading to high-temperature superconductivity is still an unsolved problem. The nature of the pairing interaction, the pairing symmetry, and whether HTS's are gapless or not are matters of extensive experimental and theoretical investigations.[8,9] Tunneling is most adequate to probe the superconducting gap and the low-energy quasiparticle excitations at the Fermi level (E_F), whereas phase-sensitive experiments are more appropriate to address the symmetry issue. Not many unquestionable fingerprints of the superconducting DOS of HTS's have emerged up to now from tunneling spectroscopy. The detailed shape of the spectra, the temperature dependence of the gap feature at E_F, and the existence of phonon-related structures are still under lively debate.[6] Experiments seem to agree on one point, which is that the reduced gap ($2\Delta/k_BT_c$) significantly exceeds the BCS weak-coupling prediction of 3.5.

Various tunneling techniques have been applied to HTS's; planar junctions,[10–12] step-edge junctions,[13] grain-boundary junctions,[14] squeezable junctions,[15] break junctions,[16–18] point-contact junctions,[19–21] and STM vacuum junctions.[22–27] The reference list given here is far from exhaustive, but it gives a general idea of the various techniques used and the different tunneling spectra obtained. All these techniques have to face the problem of the surface sensitivity of tunneling spectroscopy. Any uncertainty about the junction affects the tunneling current, and hampers an indisputable interpretation of the spectra in terms of intrinsic sample properties. Consequently, it is of primary importance to carefully check the junction quality in order to rule out, or at least identify, extrinsic barrier-related effects. The flexibility of the STM offers unique features to meet the challenge of high-quality tunneling spectroscopy. It allows an extensive *in situ* characterization of the superconductor–insulator (vacuum)–normal-metal (SIN) junction formed by the sample surface and the tip. (1) In the ideal case, the tunneling barrier consists of vacuum and the junction

0163-1829/95/51(14)/9208(11)/$06.00

area is of the order of nm^2. The junction resistance $R = V_S/I$ can be arbitrarily selected by means of the tip/sample spacing (d_{ts}), since increasing (reducing) d_{ts} increases (reduces) R. Here, V_S and I are the sample bias and the tunneling current while the STM current regulation loop is active.[7] In practice, d_{ts} is adjusted by varying V_s at constant I or vice versa. (2) The scanning capability of the STM enables the junction to be positioned at will on a subnanometer scale, allowing spatially resolved tunneling spectroscopy (STS).[28] Thereby, STM introduces high spatial resolution as a valuable complement to the high energy resolution of tunneling spectroscopy. In addition, the structural nature of the sample surface can be imaged with atomic resolution, and eventual adsorbates, atomic step structures or defects, may be observed. The mechanical stability of the STM (i.e., of the vacuum junction) and the peculiar tip-to-plane geometry might be limiting factors to its application. However, investigations of conventional superconductors in the mixed state dismiss these concerns, and demonstrate the great potential of the STM.[29,30] Experiments further established that heating effects due to the relatively high current densities through the small junction area are negligible.[26,31,32]

The experimental procedure is described in Sec. II. In Sec. III we address the problem of the SIN junction quality on BSCCO. The detailed spectroscopy and characteristic features of the DOS of BSCCO are discussed in Sec. IV.

II. EXPERIMENT

The STM (Ref. 33) and the ultrahigh-vacuum (UHV) low-temperature setup[34] we designed for the experiments discussed here have been described in previous publications. The STM features an inertial piezoelectric motor to safely approach the sample within a few angstroms of the tip.[35] A precise approach is essential to avoid mechanical damages of the sample and the tip which may compromise a good tunnel junction. The tunneling investigations were done on large $Bi_2Sr_2CaCu_2O_{8+\delta}$ single crystals (typically $3\times5\times0.05$ mm^3) grown by Mitzi *et al.*[36] using a directional solidification technique. These crystals, with doping close to optimum, have an ac susceptibility transition onset temperature $T_c = 92.3$ K with a transition width of 2.3 K. The results discussed here are representative of many experiments done over the past two years on different samples selected from the same batch. Despite its short coherence lengths ($\xi_c \leq 1$ Å, $\xi_{ab} \approx 20$ Å),[37] BSCCO is a very popular HTS for surface-sensitive investigations like tunneling spectroscopy and photoemission spectroscopy. The reason is that micrometer-sized atomically flat areas can be routinely prepared by cleaving between the weakly bonded Bi-O planes. Furthermore, the Bi-O surface exposed upon cleaving is sufficiently inert in ultrahigh vacuum as shown by photoemission.[38] We cleave the single crystals in UHV ($\sim 3\times10^{-9}$ mbar) at room temperature (RT) briefly before cooling. The cooling takes place during a slow transfer of the complete STM with tip and sample from the UHV chamber into a can immersed in liquid helium, without any exposure to air.[34] The can is filled with high-purity helium exchange gas (~ 1 mbar at RT), cryopumped to ~ 4.2 K. We found this procedure appropriate to achieve the high surface quality required for vacuum tunneling spectroscopy on BSCCO, and reproducible spectra of the superconducting DOS have been measured during up to three days after a single cleave.

Besides the sample surface, the tip is a key element in STM spectroscopy which should not be neglected in order to achieve clean junctions. We used electrochemically etched Au tips and commercial Pt/Ir tips, both giving very similar results. Each tip is conditioned by field evaporation in UHV at RT using a technique inspired by Elrod *et al.*[39] We establish a tunneling current in the range 10–100 nA for several minutes between the tip and a gold sample at negative bias above 6 V. This conditioning yields clean and stable tips.

Current-voltage $[I(V)]$ and differential conductance $[dI/dV(V)]$ curves are acquired by ramping the bias voltage while maintaining d_{ts} constant after the tip has been scanned to a specific location in constant-current mode.[40] To measure $dI/dV(V)$, we use a standard lock-in technique with a 0.5–1.0 kHz ac modulation of 0.1–1.0 mV added to the bias voltage. In first approximation, assuming the tip has a constant DOS near E_F and that the transmission of the barrier is independent of energy, the tunneling conductance is proportional to the DOS of the sample broadened by the Fermi function $f(E) = 1/\{\exp(E/k_BT)+1\}$. Thus, at low temperature,

$$\frac{dI(V)}{dV} \propto \int_{-\infty}^{+\infty} N(E) \left\{ -\frac{\partial}{\partial eV} f(E+eV) \right\} dE \cong N(eV) , \tag{1}$$

where e is the elementary charge and $N(E)$ is the DOS of the sample. The bias voltage is applied to the sample, and the origin of the energy scale in the spectra corresponds to the Fermi level of BSCCO. Hence the differential conductance at negative (positive) bias reflects the DOS below (above) E_F. BSCCO is a very anisotropic, nearly two-dimensional system, and the STM tip is mounted perpendicular to its (ab) basal plane. The tunneling current results from the finite overlap of the electron wave functions decaying into the vacuum between the two weakly interacting electrodes. Assuming a free-electron tip, it can be shown that tunneling spectroscopy in this particular geometry probes an angular average over the (ab)-plane DOS of BSCCO.[41]

III. CHARACTERIZING THE TUNNELING BARRIER

Early STM investigations of BSCCO showed that the Bi-O surface has a nonmetallic characteristic, and it was unclear whether the DOS near the Fermi level could be probed by vacuum tunneling spectroscopy.[42] We took particular care characterizing the tunneling conditions in order to achieve reproducible and relevant spectroscopy. The series of checks described below give strong evidence that clean junctions with properties representative for vacuum tunneling can be obtained on BSCCO using a STM in UHV. They emphasize that atomic resolution is

not a sufficient guarantee to probe the superconducting DOS under ideal conditions. The most constraining criteria to make sure that vacuum tunneling is achieved are spatial and temporal reproducibility of the spectra and their independence of tip/sample spacing.

Topography with atomic resolution

Figure 1 shows raw-data topographic images of two cleaved BSCCO surfaces acquired in constant-current mode[40] at 4.8 K. The (ab) plane of the orthorhombic lattice with $a \approx b = 0.54$ nm,[43] and the nearly commensurate superstructure along the **b** direction with the periodicity $4.76b$[44,45] are well resolved. The gray scale, from black to white, corresponds to a total corrugation of about 0.07 nm. Some authors concluded that vacuum tunneling conditions prevail during STM spectroscopy based on the fact that such atomic images of the surface area involved could be obtained.[23,46] This argument can only be put forward if the junction resistance R during spectroscopy is equal to or larger than R set during imaging. Indeed, increasing R after atomic imaging is equivalent to withdrawing the tip from the sample surface, and vacuum tunneling is most likely realized. On the other hand, if R is reduced to obtain spectroscopy data, d_{ts} shrinks and one cannot be certain that the tip stays clear of the sample surface.

Our investigations show that the experimental situation is not that straightforward. We find that atomic resolution is neither necessary nor sufficient to guarantee high-quality tunneling spectroscopy of the superconducting DOS of BSCCO. Sometimes clean SIN tunneling spectra can be measured even though atomic resolution is impossible to achieve in that particular run. On the other hand, low-temperature spectroscopy on surfaces which allow atomic resolution imaging shows either a superconducting [Fig. 1(a)] or a semiconducting behavior [Fig. 1(b)]. The spectra are reproducible as a function of time and location on the surface within the 4 μm range of our STM, regardless of their superconducting [Fig. 2(a)] or semiconducting [Fig. 2(b)] nature. The same single crystal shows either a semiconducting or a superconducting behavior after successive cleavages. Similar findings, where the cleaved surface of BSCCO exhibits different spectroscopic natures, were made in photoemission experiments.[47] Superconductivity in BSCCO takes place in the Cu-O planes separated by Bi-O/Sr-O layers, and the present results may give the impression that cleaving exposes either a nonmetallic Bi-O layer or a superconducting Cu-O layer. However, it seems rather unlikely that a bare Cu-O layer is superconducting. Indeed, in agreement with several independent experiments showing that BSCCO cleaves between adjacent Bi-O layers,[38,48] both surfaces in Fig. 1 are Bi-O. We draw this conclusion from the atomic rows which exhibit a similar in-plane undulation in Fig. 1(a) and Fig. 1(b). This undulation is a distinct characteristic of the Bi-O layers,[45,49] and most probably excludes the presence of a Cu-O layer at the surface. As possible explanations for the different spectroscopic characteristics measured by c-axis STM tunneling on BSCCO, it has been argued that the superconducting DOS is probed through defects in the Bi-O surface[50] or at step edges which expose Cu-O layers.[11,22,51] The spatial reproducibility we achieve[52] (see also Fig. 6 below) and the atomically flat surface imaged in Fig. 1(a) disclaim these two arguments.

We suggest that the distinct spectroscopic signatures observed on BSCCO (Fig. 2) are due to changing characteristics of the surface layer, like, for example, the oxygen stoichiometry, which determine whether the underlying topmost Cu-O layer is superconducting or not. In this picture, the $I(V)$ curve in Fig. 2(a) corresponds to a situation where the topmost Cu-O layer is superconducting. The way the linear branches extrapolate to zero current excludes a Coulomb blockade as the origin of the gap at zero bias.[53] The linearity at high bias, and the fact that this $I(V)$ curve was measured at a larger d_{ts}($R = 2.0$

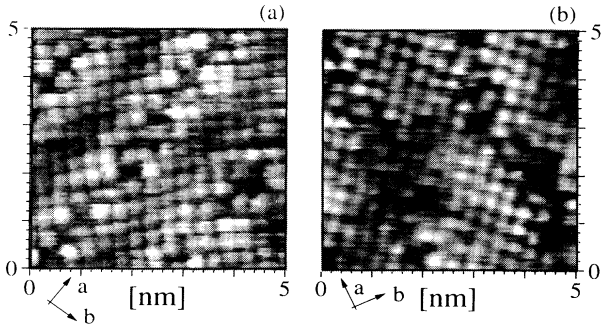

FIG. 1. Constant-current STM topographic images of *in situ* cleaved $Bi_2Sr_2CaCu_2O_{8+\delta}$ single crystals at 4.8 K (raw data). (a) Surface which shows a superconducting gap (imaging parameters: $I = 275$ pA, $V_s = 0.5$ V, $R = 1.8$ GΩ). (b) Surface which shows a semiconducting gap ($I = 300$ pA, $V_s = 0.5$ V, $R = 1.7$ GΩ).

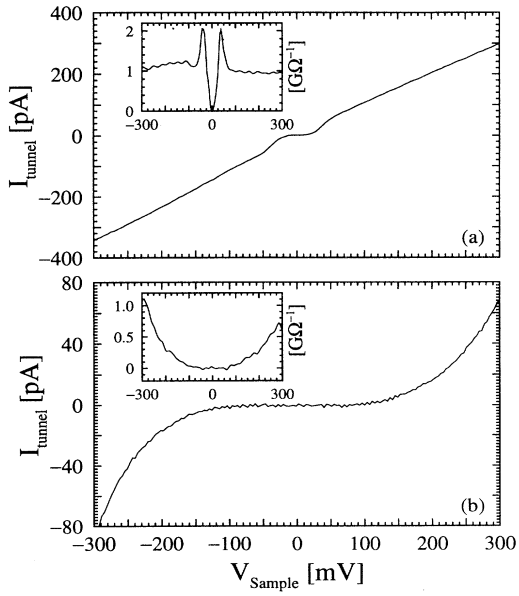

FIG. 2. $I(V)$ characteristics of $Bi_2Sr_2CaCu_2O_{8+\delta}$ at 4.8 K (Au tip). The numerical derivative of each $I(V)$ curve is shown in the inset. (a) Acquired in the region of Fig. 1(a) with $R = 2.0$ GΩ. (b) Acquired in the region of Fig. 1(b), with $R = 1.0$ GΩ.

GΩ) than the preceding atomic imaging [Fig. 1(a), $R = 1.8$ GΩ], are strong hints for a nearly ideal vacuum barrier between the tip and the Bi-O surface. Note that tunneling in this case shows the sharpest and best developed superconducting gap feature [Fig. 3(a)], the highest reproducibility as a function of time and position on the sample, and that the spectra are independent of d_{ts} (Ref. 27) [see also Figs. 4(a) and 5 below). We conclude that here the STM probes the intrinsic DOS of the topmost Cu-O layer by tunneling through vacuum plus the Bi-O/Sr-O surface layer, which is presumably nonmetallic.[54] Accordingly, we believe that the spectra shown in Fig. 2(b) correspond to a situation with a nonsuperconducting topmost Cu-O layer. In this case, the STM measures a semiconductinglike gap, and approaching the tip closer to the surface (R is smaller during spectroscopy than during topography) does not reveal any trace of superconductivity, unless a point contact is achieved [Fig. 3(b)]. The spectra obtained under such point-contact conditions are not reproducible from junction to junction. Furthermore, they do not systematically reflect a superconducting gap. We think that a degraded surface with off-stoichiometric composition or with defects prevents superconductivity in the topmost Cu-O layer. The tip needs then to be pushed into the sample to probe the DOS of deeper-lying superconducting Cu-O layers. The larger number of atomic defects in Fig. 1(b) compared to Fig. 1(a) is consistent with the idea of a degraded surface stoichiometry. Unfortunately, the corrugation features in these figures are consistent with the Bi sublattice as well as the O sublattice of about 0.38 nm.[43] Therefore it is not possible to affirm that oxygen vacancies in the surface layer are responsible for the nonsuperconducting topmost Cu-O layer, leaving this question open.

We sometimes observe a third situation where vacuum tunneling is hindered by a contamination of the Bi-O surface [Fig. 3(c)]. In this case, the tip needs to be brought close to the surface, but not in point contact, to probe the DOS of the Cu-O layer. The tunneling current is then likely to be affected by leakage currents through the contamination, which lead to an unusual background conductance and a smeared gap feature at E_F. Moreover, if the tip is very close to the surface, the tunneling current may be altered by a deformed overbiased tunneling barrier, or/and a Coulomb blockade. The first effect results in a parabolically increasing background conductance as a function of bias voltage. The Coulomb blockade yields an artificially low conductance at zero bias, which may simulate a completely gapped Fermi surface, even in the case of a gapless superconductor. For the two nonvacuum tunneling conditions illustrated in Figs. 3(b) and 3(c), we find poor reproducibility of the tunneling characteristics, the peaks at the superconducting gap edges ($\pm\Delta_p$) are not well developed, and the spectra are strongly d_{ts} dependent [Fig. 4(b)]. The tunneling spectra obtained from such junctions certainly do not reflect the intrinsic superconducting DOS of BSCCO, and, in particular, sub-

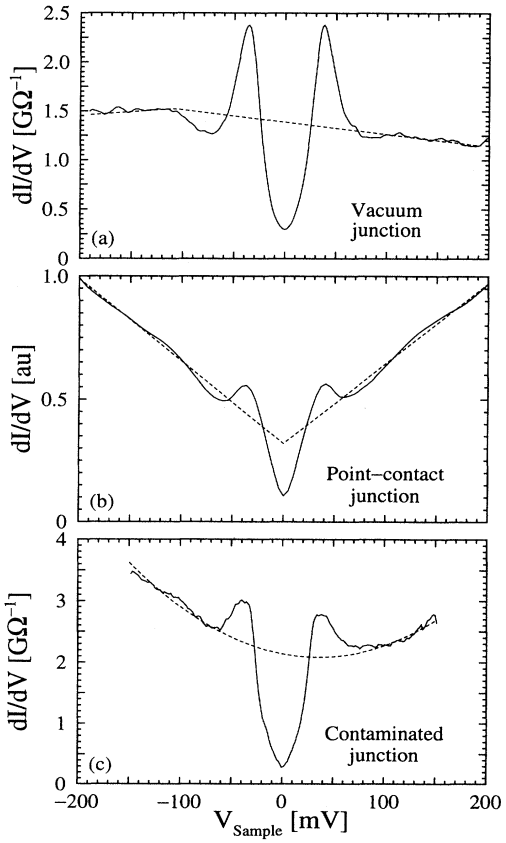

FIG. 3. Differential SIN conductance spectra measured for different junction qualities at 4.8 K using a gold tip. The dashed line represents the extrapolated normal-state conductance (N'IN junction). (a) Vacuum tunnel junction, $R = 0.6$ GΩ. (b) Point-contact junction, $R < 0.03$ GΩ. (c) Contaminated tunnel junction, $R = 0.3$ GΩ.

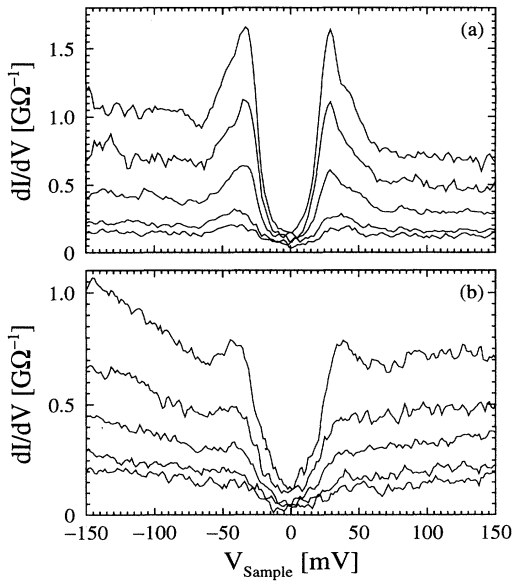

FIG. 4. Differential conductance spectra measured as a function of tip/sample spacing at 4.8 K using a gold tip. The voltage is changed from 0.3 V (top spectrum) to 0.7 V (bottom spectrum) with 0.1 V increments at constant $I = 0.3$ nA. (a) Vacuum junction. (b) Degraded junction.

stantial background corrections are required to extract the DOS from the experimental data. Unlike spectra obtained with clean vacuum junctions, which do not fit to a BCS-like isotropic gap parameter [Fig. 3(a)], spectra measured with a nonideal junction are apparently in reasonably good agreement with a standard BCS density of states if an important and presumably unphysical amount of pair breaking is assumed. In this case, the non-BCS features seen in the cleaner spectra are washed out by the experimental broadening. These contradictory behaviors demonstrate the importance of carefully checked tunneling conditions to remove such ambiguities.

Tip/sample distance dependence of the tunneling spectra

The d_{ts} dependence of the spectra is a meaningful check of the junction quality. In each set of spectra illustrated in Fig. 4(a) and 4(b), d_{ts} was increased by increasing the bias voltage from 0.3 to 0.7 V at constant 0.3 nA tunneling current (top spectrum to bottom spectrum). In Fig. 4(a), the gap remains well developed at any voltage as expected for vacuum tunneling. In Fig. 4(b), the peaks at $\pm\Delta_p$ are weaker and disappear at high bias (large d_{ts}), which we ascribe to tunneling through a contaminated junction. The independence of the tunneling spectra on d_{ts} under vacuum tunneling conditions[26,27] is even better demonstrated in Fig. 5. Here, d_{ts} was increased by reducing the tunneling current from 1.0 to 0.2 nA at constant 0.4 V sample bias [Fig. 5(a) top spectrum to bottom spectrum]. These spectra fit onto one single curve in a normalized conductance scale [Fig. 5(b)], which is a clear signature of a clean vacuum tunnel junction. The quality of each junction can be quantified by the apparent work function ϕ defined as $\sqrt{\phi} \propto d\ln I_t / dd_{ts}$. The ϕ measured by STM is often lower than the work function of a bare surface, and it decreases as R is reduced.[42] This behavior is a consequence of a lowered surface barrier induced by the close proximity of tip and sample. We find $\phi > 0.2$ eV for good junctions as in Figs. 4(a) and 5, and $\phi \approx 0.01$ eV for contaminated junctions as in Fig. 4(b). The magnitude of ϕ drops below 1 meV for junctions with a semiconducting characteristic [Fig. 2(b)]. Although the low values found by STM are still a puzzling problem, the vanishing ϕ clearly indicates a degradation of the junctions in Fig. 4(b) compared to Figs. 4(a) and 5. These experiments show that a nearly ideal vacuum junction is achieved if sharp superconducting spectra as in Fig. 3(a) can be measured at high R, and thus at a d_{ts} large enough that we are sure not to touch the sample surface with the tip. This analysis does not mean that high-R junctions are restricted to high-ϕ surfaces, but it tells us that the superconducting DOS is obscured by artefacts in degraded junctions (small ϕ), and cannot be observed properly either at high or at low R.

We observe three characteristic background conductances in STM spectroscopy on BSCCO illustrated as dashed lines in Fig. 3. The most reproducible spectra, showing a well developed superconducting gap with the sharpest features at $\pm\Delta_p$, always exhibit the flattest background conductance [Fig. 3(a)]. Figure 2 in Ref. 26 shows the same correlation between sharp gap features

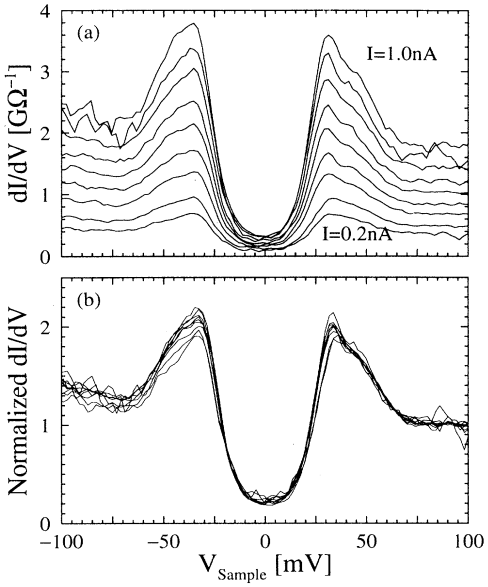

FIG. 5. Differential conductance spectra measured as a function of tip/sample spacing with a clean vacuum junction (4.8 K, gold tip). (a) The tunneling current is changed from 1.0 nA (top spectrum) to 0.2 nA (bottom spectrum) with 0.1 nA increments at constant $V_s = 0.4$ V. (b) Same curves plotted on a normalized conductance scale to demonstrate their independence of d_{ts}.

and a constant background conductance. The linearly[10,16,20,24,25,55] [Fig. 3(b)] and the parabolically[50,56] [Fig. 3(c)] increasing backgrounds are often reported in the literature as intrinsic features of tunneling spectra on BSCCO and other HTS's. In contrast to this statement, the present results clearly indicate that neither a V-shaped nor a parabolic background conductance is intrinsic to tunneling spectroscopy of BSCCO. Our data also firmly demonstrate that there is no intrinsic d_{ts} dependence[57] of the spectra. We find a strong correlation between the presence of the extrinsic V-shaped or parabolic background conductance and the occurrence of a d_{ts} dependence of the spectra. These two behaviors show up simultaneously, whenever a low R is required to sense the superconducting DOS of BSCCO. According to the above discussion, both appear as artefacts of nonideal vacuum junctions, where the tip needs to be driven close to the surface with the risk of touching it.

Scanning tunneling spectroscopy

Spatial reproducibility of the spectra at low temperature is a further signature of ideal vacuum tunneling conditions. Figure 6 shows a series of differential conductance spectra measured every 0.625 nm along a 34 nm path at 4.8 K. Each conductance curve is an average of two spectra. The limited capacity of the helium vessel did not allow enough time for more averaging which would reduce the noise level. The spectra in Fig. 6(a) are displaced vertically as a function of scan distance, while the same data are plotted without a vertical shift in Fig.

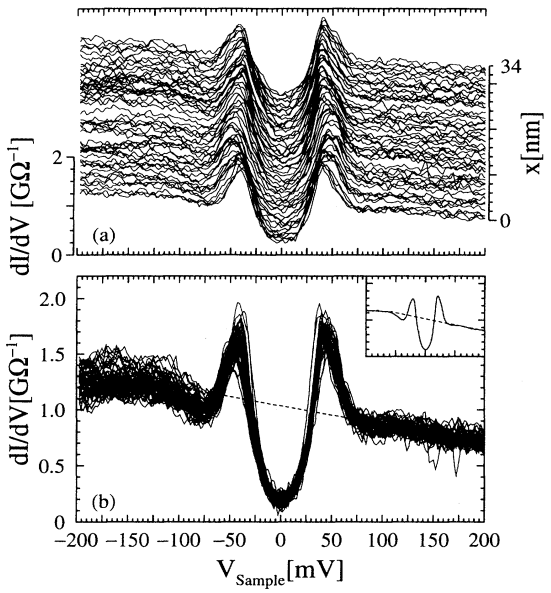

FIG. 6. Differential conductance spectra measured along a 34 nm path at 4.8 K (Au tip, $R=1.0$ GΩ). Note the absolute conductance scale and the nearly Ohmic background conductance, both signatures of a high-quality vacuum junction in each location. (a) The spectra are displaced vertically as a function of position. (b) The spectra are plotted on top of each other. The inset shows their numeric average, and the dashed line represents the normal-state conductance obtained from a linear extrapolation of the background conductance.

6(b). The tip is scanned between spectroscopic measurements with constant 0.4 nA tunneling current at 0.4 V sample bias. Hence the active feedback loop junction resistance equals $R=1.0$ GΩ, in good agreement with the average resistivity extracted from the spectra. This means the background conductance is close to Ohmic up to 0.4 eV. Note the absolute conductance scale, indicating that the spectra have not been normalized. The remarkable reproducibility of the background conductance as a function of position is strong evidence for homogeneous and ideal junctions formed along the 34 nm path. Such results are exclusively obtained when clean vacuum tunneling as described above is achieved.

Despite the low averaging, the spectra are only weakly scattered. They reflect the general features of higher-resolution data discussed in Sec. IV. The background conductance is largely constant and the superconducting gap is well developed. Even the dip feature at negative sample bias is resolved, as shown in the spectrum obtained by averaging all spectra displayed in Fig. 6 [Fig. 6(b), inset]. Note the more pronounced conductance scattering at negative sample bias compared to positive bias. This difference is certainly related to the difficulty in obtaining good topographic images at negative sample bias.[58] It may be a signature of a particular mechanism involved when electrons tunnel out of BSCCO (at negative sample bias), which could be related to high-temperature superconductivity.

IV. VACUUM TUNNELING SPECTROSCOPY OF $Bi_2Sr_2CaCu_2O_{8+\delta}$

In Sec. III, we demonstrated that relevant c-axis vacuum tunneling spectroscopy of BSCCO can be achieved in careful STM experiments. We focus now on typical spectra obtained with such well characterized SIN junctions. Figure 7 shows a differential conductance spectrum and an $I(V)$ curve measured at 4.8 K in two separate experiments. The $dI/dV(V)$ curve shows a well developed superconducting gap at E_F with large peaks at the gap edges ($\pm\Delta_p$), and a finite density of quasiparticle excitations filling the gap. Among remarkable features, we note a striking asymmetry with respect to E_F, with a dip which reproducibly appears beyond the superconducting gap at negative sample bias only. The background conductance is essentially Ohmic with a slight decrease with increasing bias voltage up to ±300 meV. This result disclaims the statement that the frequently measured V-shaped or parabolic background conductance is intrinsic to tunneling on HTS's, at least for BSCCO. Moreover, such increasing background conductances obscure the dip feature we systematically observe at negative sample bias. This is nicely seen in Fig. 3. The slope of the $I(V)$ curve is steeper at negative sample bias than at positive bias [see also Fig. 2(a)], which may reflect a slight electron-hole asymmetry in the DOS of BSCCO. The spectra remain essentially unchanged, whether we use a gold tip or a Pt/Ir tip. The general aspect of the spectra does not change if a magnetic field up to 1.5 T is applied perpendicular to the (ab) basal plane.

The *background conductance* refers to the differential conductance at $|V_S| \gg \Delta/e$ in the superconducting state. This part of the spectra is expected to be largely independent of whether BSCCO is superconducting (SIN junction) or not (N'IN junction, where N' stands for BSCCO in the normal state). Therefore one can estimate a N'IN spectrum by extrapolating the SIN background conductance into the superconducting gap. The N'IN conductance plotted as a dashed line in Figs. 7 and 3(a) results from a linear extrapolation of the SIN background con-

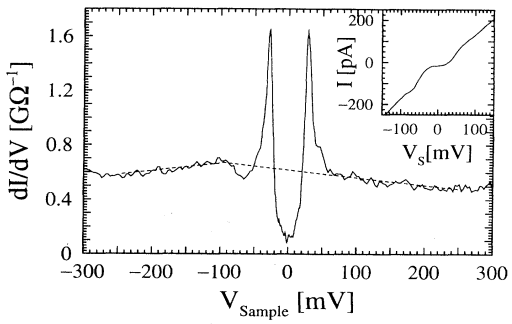

FIG. 7. Vacuum tunneling differential conductance spectrum of superconducting $Bi_2Sr_2CaCu_2O_{8+\delta}$ at 4.8 K (Au tip, $R=1.5$ GΩ). We used a lower time constant below ±50 meV to increase the resolution (Ref. 61). The dashed line represents the normal-state conductance estimated from a linear extrapolation of the background. The inset shows an independently measured $I(V)$ curve (Au tip, $R=0.7$ GΩ).

ductance up to ±300 meV. It has a maximum at negative sample bias, indicating that the (*ab*)-plane normal-state DOS of BSCCO is peaked below the Fermi level. We performed preliminary tunneling experiments at $T > T_c$ (Fig. 8), which confirm the main features of the normal-state conductance deduced from the above coarse extrapolation. The spectra shown in Fig. 8 were acquired on the same sample at $T = 4.8$ K (SIN, solid line) and $T \approx 115$ K (N'IN, dashed line) during two separate experiments. The N'IN curve was normalized in order to match the R of the SIN junction. The position of the maximum in the N'IN curve is in the range 70–100 meV below E_F. Normal-state conductances that are peaked near E_F have been reported earlier from point-contact[21,59] and break-junction[18] tunneling experiments, though without pointing out the marked asymmetry we observe with respect to E_F. Moreover, Huang *et al.*[21] observe the decreasing background conductance only for point-contact junctions with $R < 10$ kΩ, whereas in their experiments it becomes increasing for higher-R junctions. Hence there is the possibility that the decreasing background they find is due to a metallic contribution to the tunneling current as described by Blonder, Tinkham, and Klapwijk.[60] In our experiments, we measure a reproducible decreasing background conductance even for junctions with $R > 1.0$ GΩ, where only vacuum tunneling contributes to the measured conductance. Therefore, the experimental conductance curves presented in Fig. 8 without any background corrections do most likely reflect real DOS features of BSCCO. Note that the SIN spectrum shown in Fig. 8 was acquired with a longer time constant than the spectrum in Fig. 7; thus the apparent broadening of the gap feature is experimental, due to a lower energy resolution.[61]

The conservation of states between normal and superconducting BSCCO is an important issue. The integration over energy of the extrapolated N'IN spectrum and the experimental SIN spectrum in Fig. 7 yields the same number of states. To our knowledge, this is the first time that this sum rule has been verified for a HTS in vacuum tunneling spectroscopy, without any background conductance corrections. The experimental spectra presented in Fig. 8 also satisfy this sum rule. Taking the dashed line as the normal-state conductance in Fig. 3, the sum rule is verified for a vacuum junction [Fig. 3(a)], but neither for point-contact [Fig. 3(b)] nor for contaminated junctions [Fig. 3(c)]. The last two cases show an excess of states in the normal state. This is expected if the measured gap is not purely due to superconductivity, when, for example, a Coulomb blockade contributes to the tunneling process. These results give us additional confidence that Figs. 7 and 8 illustrate the intrinsic (*ab*)-plane DOS of BSCCO.

The characteristic features of the tunneling spectra discussed here are consistent with break-junction[17,18] experiments and angular-resolved photoemission spectroscopy (ARPES). ARPES data reveal a broadband[62] and a dip[63] below the gap in the occupied DOS of BSCCO, in good correspondence with structures present at negative sample bias in the differential conductance spectra discussed here. Our SIN tunneling data can be directly compared to break-junction SIS spectra [$dI/dV_{\mathrm{SIS}}(V)$] using the expression

$$dI/dV_{\mathrm{SIS}}(V) \propto N(-eV)N(0) + \int_0^{eV} N(\varepsilon - eV)[dN(\varepsilon)/d\varepsilon]d\varepsilon \ , \quad (2)$$

where the DOS of the normal-metal electrode is assumed to be constant, and $N(E)$ is the DOS of the superconducting electrode (i.e., BSCCO). To compute the SIS conductance curve shown in Fig. 9(a), $N(E)$ was approximated by the experimental $dI/dV(V)$ curve in Fig. 7 (solid line). The calculated spectrum is in remarkable agreement with the 5 K break-junction data of Mandrus *et al.*[18] The same comparison between STM tunneling and break-junction tunneling can be made for BSCCO in the normal state at $T > T_c$. The N'IN' spectrum shown in Fig. 9(b) was computed using Eq. (2) and approximat-

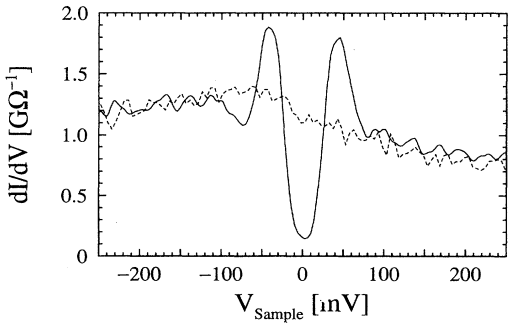

FIG. 8. Vacuum tunneling differential conductance spectra of $Bi_2Sr_2CaCu_2O_{8+\delta}$ (Pt/Ir tip, $R = 1.1$ GΩ), at 4.8 K in the superconducting state (solid line), and above T_c, in the normal state (dashed line).

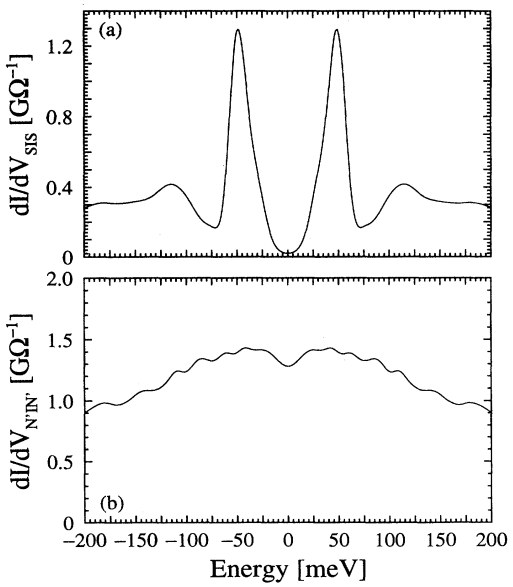

FIG. 9. Numerical break-junction spectra computed using Eq. (2). (a) BSCCO in the superconducting state, based on the $dI/dV(V)$ curve measured at 4.8 K in Fig. 7. (b) BSCCO in the normal state, based on the $dI/dV(V)$ curve measured above T_c in Fig. 8.

ing $N(E)$ by the N'IN differential conductance curve measured by STM on BSCCO at $T > T_c$ (Fig. 8, dashed line). Again, the resulting spectrum is in excellent agreement with data of Mandrus *et al.*[64] In particular, the numerical spectrum in Fig. 9(b) reproduces the weak dip at zero bias which is present in the 100 and 135 K spectra of Mandrus *et al.*[64] (i.e., at $T > T_c$). Hence what might be interpreted as a reminiscence of the superconducting gap above T_c in break-junction experiments can be explained in terms of the asymmetric peaked normal-state DOS of BSCCO we observe by STM.[65]

The above results support the idea that *c*-axis tunneling spectroscopy probes the (*ab*)-plane density of states of BSCCO. Break-junction tunneling does not have the bias polarity sensitivity of SIN tunneling. Break junctions are unable to differentiate states below E_F from states above E_F, and the spectra are symmetric with respect to E_F. Consequently, Mandrus *et al.*[18] observe the dip structure on both sides of the superconducting gap, and they postulate that the normal-state DOS has a maximum at E_F. The tunneling spectra we obtain by STM yield a different, very asymmetric DOS. The normal-state DOS is peaked below E_F, and the dip at about -70 meV in the superconducting DOS appears only at negative sample bias (Fig. 7). Figure 6(b) unambiguously shows that there is no dip at positive sample bias outside the superconducting gap. Similar dip features beyond the superconducting gap have been reported from earlier SIN tunneling experiments,[11,22,66] though without the reproducibility demonstrated here, and without pointing out its absence at positive sample bias. Temperature-dependent photoemission[63] and break-junction[18,64] experiments indicate that the dip beyond the gap disappears as the temperature is raised above T_c. Hence it seems related to the superconducting state of BSCCO. We do not yet have a complete set of temperature-dependent data, but our N'IN spectra (Fig. 8) show that the dip is indeed absent 23 K above T_c. Figures 7 and 8 nicely illustrate how the states are redistributed below T_c, giving rise to the superconducting gap and the dip beyond the gap. The fact that the dip contributes a significant amount of states to satisfy the sum rule suggests that this feature is indeed related to the superconducting state of BSCCO. We believe that the absence of the dip at positive sample bias in SIN spectra deserves particular attention. This asymmetry may contain essential information on the superconducting state of BSCCO, and it could be a particular constraint on theoretical models of HTS's.[67] If the dip is interpreted as a phonon structure, its absence at positive bias tunneling needs to be explained.

The low-bias tunneling conductance holds valuable information on the superconducting state. It allows a direct measure of the superconducting gap parameter Δ. In the absence of an established model of HTS's, we define Δ as the intersection of the background conductance with the gap feature. Applying this definition to the data in Fig. 6(b), we find $\Delta = 29.5 \pm 4$ meV. Considering a T_c of 92.3 K, the reduced gap equals $2\Delta/k_B T_c = 7.4 \pm 1$, in close agreement with other experiments on BSCCO. Note that if the *d*-wave or extended *s*-wave interpretation considered below is correct without pair breaking, the maximum gap is to be taken at the peak of the superconducting DOS, and would thus be 5–10 meV larger.

In all our SIN spectra, the zero-bias conductance is in the range of 8%–20% of the normal-state conductance. Contrary to the asymmetry observed outside the superconducting gap, we find that the peaks at $\pm\Delta_p$ are comparable, and, although there are slight changes between different spectra, there is no significant asymmetry in this part of the spectra. In particular, we do not observe any systematic asymmetry in the peak height at $\pm\Delta_p$ which could reflect an electron-hole asymmetry as recently suggested by Hirsch.[68] A simple BCS density of states does not fit the experimental differential conductance curve, even if some pair breaking is accounted for. The dashed-dotted curve in Fig. 10 was computed using the phenomenological Dynes, Narayanamurti, and Garno[69] DOS given by

$$N(E) = \mathrm{Re}\{|E - i\Gamma| / [(E - i\Gamma)^2 - \Delta^2]^{1/2}\} ,$$

where Re stands for the real part and Γ is the pair-breaking strength. The fit was adjusted to match the height of the peaks at $\pm\Delta_p$, the fitting parameters being $\Gamma = 0.7$ meV and $\Delta = 27.5$ meV. The experimental curve measures many more states in the gap than predicted by this BCS curve. Any larger lifetime parameter Γ necessary to fit the spectrum near E_F fails to fit the spectrum at $\pm\Delta_p$.

The gap feature we observe in clean vacuum tunneling spectra may reflect an anisotropic gap parameter (Δ_k). In the following we discuss our spectra in the framework of $d_{x^2-y^2}$ symmetry. However, since SIN tunneling is not sensitive to the sign of Δ, the following arguments would as well apply to an extended *s*-wave symmetry or any equivalent distribution of the magnitude of the gap parameter. Applying the maximum-entropy filtering technique (MaxEnt) to our data, we found a Δ_k consistent with a $d_{x^2-y^2}$ symmetry.[70] The asymptotic conductance predicted for a $d_{x^2-y^2}$ symmetry close to E_F (Fig. 10, dashed line) is given by $\sigma_d(V) = \sigma_n eV/\Delta_p$, where σ_n is the normal-state conductance. The low-bias conductance

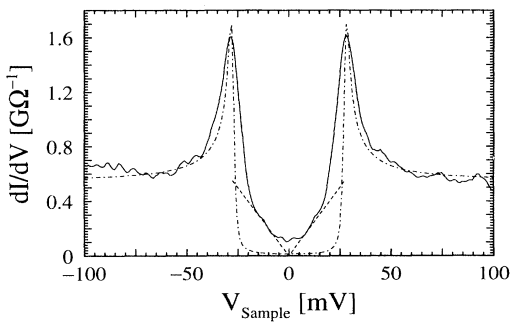

FIG. 10. Differential conductance spectrum (Au tip, $R = 1.5$ GΩ) of superconducting $Bi_2Sr_2CaCu_2O_{8+\delta}$ measured at 4.8 K (solid line). BCS fit with a pair-breaking contribution: $\Gamma = 0.7$ meV, $\Delta = 27.5$ meV (dashed-dotted line). Asymptotic low-bias behavior predicted for a *d*-wave symmetry: $dI/dV(V) \propto \sigma_n eV/\Delta_p$ (dashed line).

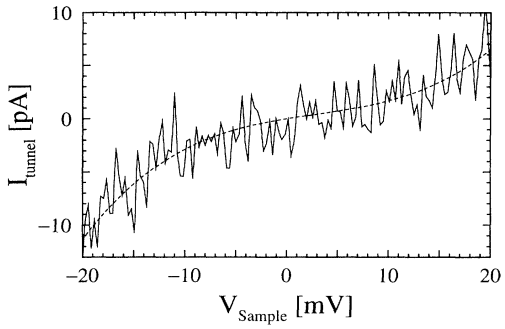

FIG. 11. High-resolution $I(V)$ curve on $Bi_2Sr_2CaCu_2O_{8+\delta}$ at 4.8 K (Au tip, $R=0.75$ GΩ). The dashed line corresponds to a third-order polynomial least-squares fit.

we measure follows this asymptotic behavior quite well. Thus our data are close to what would be expected for a d-wave gap parameter. However, there are also some discrepancies with such a symmetry. In particular, the peaks at $\pm\Delta_p$ are broader and up to 50% higher than predicted for a d-wave symmetry.[71] The rounding of the $dI/dV(V)$ curve near E_F is either intrinsic or due to scattering effects in the material. To investigate this region of the spectrum more carefully, we measured $I(V)$ curves without the ac modulation required for differential conductance measurements (Fig. 11). These curves show a dominating $I \propto V^3$ plus an $I \propto V^2$ dependence of the tunneling current on bias voltage as illustrated by the least-squares fit plotted in Fig. 11 (dashed line). These experiments exclude the possibility that leakage currents are responsible for the finite DOS measured in the gap, since we observe no significant linear ($I \propto V$) contribution at zero bias. Furthermore, this result indicates that, if there is a minimum gap as expected in the case of an anisotropic s-wave gap, it has to be smaller than $2\Delta_{min}=4$ meV. This value corresponds to the smallest gaplike feature we could identify at E_F in a numerical differentiation of the $I(V)$ curve shown in Fig. 11.

At the present stage, despite the very clean tunneling characteristics, we cannot make any stronger statement about the symmetry of Δ_k. The difficulty is that SIN spectroscopy is not sensitive to the phase of the gap parameter. In particular, different gap symmetries where the amplitude $|\Delta_k|$ follows similar distributions but with distinct phases may produce similar features in the $I(V)$ characteristics. A more detailed investigation of this exciting issue by STM is certainly to come in the near future from spatially resolved tunneling spectroscopy in the vicinity of a defect or a vortex line. Specific DOS patterns depending on Δ_k have been predicted around such regions which locally depress superconductivity.[72]

V. SUMMARY

We have demonstrated that clean c-axis vacuum tunneling spectroscopy on cleaved BSCCO single crystals can be achieved in careful STM experiments in an UHV environment. We achieved very reproducible tunneling spectroscopy at 4.8 K. Vacuum tunneling differential conductance curves exhibit sharp peaks at the gap edges and a finite density of quasiparticle excitations filling the gap. We found that neither a V-shaped nor a parabolic background conductance nor any tip/sample distance dependence of the spectra are intrinsic features of tunneling spectroscopy of BSCCO. These features appear related to degraded tunneling barriers, where only low-resistance junctions reveal a trace of the superconducting energy gap. They correspond to the most unstable and less reproducible tunneling conditions.

An important result of this work is the striking asymmetry of the DOS with respect to the Fermi level. The normal-state conductance has a maximum in the range -70 to -100 meV sample bias, which indicates that the (ab)-plane normal-state DOS is peaked below the Fermi level. Differential conductance spectra measured below T_c reveal a dip feature at about -70 meV outside the superconducting gap which systematically appears only at negative sample bias. We believe this asymmetry deserves particular attention since it is likely to contain essential information on the high-temperature superconducting state. In the discussion we evidenced three independent experimental techniques (STM tunneling, break-junction tunneling, and photoemission) which reveal these features in the DOS of BSCCO. This remarkable consistency excludes experimental artefacts as the origin of the dip. Another important result of this work is the conservation of states we found between normal and superconducting BSCCO. To our knowledge, this is the first time that this sum rule has been verified for a HTS based on SIN experiments without any correction of the spectra. Note that the dip feature mentioned above seems to contribute a substantial amount of states to satisfy this sum rule. This is a strong sign that the dip is indeed related to the superconducting state of BSCCO.

The tunneling spectra unambiguously reveal a finite quasiparticle DOS in the superconducting gap. This result is not consistent with an isotropic BCS-like s-wave gap parameter. The MaxEnt analysis and the asymptotic behavior of the low-bias conductance suggest a $d_{x^2-y^2}$ or extended s-wave symmetry of the order parameter. However, there are distinct features, like the width and the height of the conductance peaks at the gap edges, which do not fit the prediction of these models. In addition, tunneling spectroscopy is not sensitive to the sign of Δ_k, and thus is unable to differentiate gap symmetries which differ only by their phase but which have similar amplitude distributions. Hence tunneling spectroscopy does not have the appropriate sensitivity to completely resolve the symmetry of Δ_k. However, there are theoretical predictions of particular DOS patterns in the vicinity of a region where superconductivity is depressed very locally, which depend on the gap symmetry. The high-quality vacuum tunnel junctions demonstrated in this work are a first step towards spatially resolved tunneling spectroscopy required to verify these theoretical predictions.

ACKNOWLEDGMENTS

We thank D. B. Mitzi, L. W. Lombardo, and A. Kapitulnik for providing the $Bi_2Sr_2CaCu_2O_{8+\delta}$ single crystals. We are also grateful to J.-G. Bosch for his very efficient technical assistance. This work was supported by the Swiss National Science Foundation.

[1]I. Giaever, Phys. Rev. Lett. **5**, 147 (1960); **5**, 464 (1960).
[2]J. C. Fisher and I. Giaever, J. Appl. Phys. **32**, 172 (1961).
[3]J. Nicol, S. Shapiro, and P. H. Smith, Phys. Rev. Lett. **5**, 461 (1960).
[4]For example, E. L. Wolf, *Principles of electron tunneling spectroscopy* (Oxford University Press, New York, 1985).
[5]For example, R. Meservey and B. B. Schwartz, in *Superconductivity,* edited by R. D. Parks (Dekker, New York, 1969); W. L. McMillan and J. M. Rowell, *ibid.*, and references therein.
[6]For reviews, see, e.g., J. R. Kirtley, Int. J. Mod. Phys. B **4**, 201 (1990); T. Hasegawa, H, Ikuta, and K. Kitazawa, in *Physical Properties of High Temperature Superconductors,* edited by D. M. Ginsberg (World Scientific, Singapore 1992), Vol. III, p. 525; P. J. M. van Bentum and H. van Kempen, in *Scanning Tunneling Microscopy I,* Vol. 20 of *Springer Series in Surface Sciences,* edited by H.-J. Güntherodt and R. Wiesendanger (Springer-Verlag, Berlin, 1992).
[7]G. Binnig, H. Rohrer, Ch. Gerber, and E. Weibel, Phys. Rev. Lett. **49**, 57 (1982).
[8]For recent reviews, see R. C. Dynes, Solid State Commun. **92**, 53 (1994); J. R. Schrieffer, *ibid.* **92**, 129 (1994).
[9]V. Z. Kresin and S. A. Wolf, J. Supercond. **7**, 865 (1994); D. J. Scalapino, Phys. Rep. **250**, 329 (1995).
[10]H. Ikuta, A. Maeda, K. Uchinokura, and S. Tanaka, Jpn. J. Appl. Phys. **6**, L1038 (1988).
[11]H. J. Tao, A. Chang, Farun Lu, and E. L. Wolf, Phys. Rev. B **45**, 10 622 (1992).
[12]A. G. Sun, D. A. Gajewski, M. B. Maple, and R. C. Dynes, Phys. Rev. Lett. **72**, 2267 (1994).
[13]R. B. Laibowitz, R. P. Robertazzi, R. H. Koch, A. Kleinsasser, J. R. Kirtley, J. M. Viggiano, R. L. Sandstrom, and W. J. Gallagher, Phys. Rev. B **46**, 14 830 (1992).
[14]P. Chaudhari, J. Mannhart, D. Dimos, C. C. Tsuei, J. Chi, M. M. Oprysko, and M. Scheuermann, Phys. Rev. Lett. **60**, 1653 (1988); A. Kussmaul, E. S. Hellman, E. H. Hartford, Jr., and P. M. Tedrow, Appl. Phys. Lett. **63**, 2824 (1993).
[15]T. Walsh, J. Moreland, R. H. Ono, and T. S. Kalkur, Phys. Rev. Lett. **66**, 516 (1991).
[16]J. Moreland, J. W. Ekin, L. F. Goodrich, T. E. Capobianco, A. F. Clark, J. Kwo, M. Hong, and S. H. Liou, Phys. Rev. B **35**, 8856 (1987).
[17]Th. Becherer, J. Kowalewski, M. Schmitt, M. Huth, W. Assmus, and H. Adrian, Z. Phys. B **86**, 23 (1992).
[18]D. Mandrus, J. Hartge, C. Kendziora, L. Mihaly, and L. Forro, Europhys. Lett. **22**, 199 (1993).
[19]S. Vieira, M. A. Ramos, M. Vallet-Regi, and J. M. Gonzalez-Calbet, Phys. Rev. B **38**, 9295 (1988).
[20]T. Ekino and J. Akimitsu, Phys. Rev. B **40**, 6902 (1989).
[21]Q. Huang, J. F. Zasadzinski, K. E. Gray, J. Z. Liu, and H. Claus, Phys. Rev. B **40**, 9366 (1989).
[22]J.-X. Liu, J.-C. Wan, A. M. Goldman, Y. C. Chang, and P. Z. Jiang, Phys. Rev. Lett. **67**, 2195 (1991).
[23]T. Hasegawa, M. Nantoh, and K. Kitazawa, Jpn. J. Appl. Phys. **30**, L276 (1991).
[24]J. Kane, Q. Chen, K.-W. Ng, and H.-J. Tao, Phys. Rev. Lett. **72**, 128 (1994).
[25]J. Liu, Y. Li, and C. M. Lieber, Phys. Rev. B **49**, 6234 (1994).
[26]E. L. Wolf, A. Chang, Z. Y. Rong, Yu. M. Ivanchenko, and Farun Lu, J. Supercond. **7**, 355 (1994).
[27]Ch. Renner, Ø. Fischer, A. D. Kent, D. B. Mitzi, and A. Kapitulnik, Physica B **194–196**, 1689 (1994).
[28]S. A. Elrod, A. L. de Lozanne, and C. F. Quate, Appl. Phys. Lett. **45**, 1240 (1984).
[29]H. F. Hess, R. B. Robinson, R. C. Dynes, J. M. Valles, Jr., and J. V. Waszczak, Phys. Rev. Lett. **62**, 214 (1989).
[30]Ch. Renner, A. D. Kent, Ph. Niedermann, and Ø. Fischer, Phys. Rev. Lett. **67**, 1650 (1991).
[31]H. F. Hess, R. B. Robinson, R. C. Dynes, J. M. Valles, Jr., and J. V. Waszczak, J. Vac. Sci. Technol. A **8**, 450 (1990).
[32]Q. Huang, J. F. Zasadzinski, and K. E. Gray, Phys. Rev. B **42**, 7953 (1990).
[33]Ch. Renner, Ph. Niedermann, A. D. Kent, and Ø. Fischer, J. Vac. Sci. Technol. A **8**, 330 (1990).
[34]A. D. Kent, Ch. Renner, Ph. Niedermann, and Ø. Fischer, Ultramicroscopy **42–44**, 1632 (1992). Recent improvements include an *in situ* sample and tip transfer mechanism.
[35]Ch. Renner, Ph. Niedermann, A. D. Kent, and Ø. Fischer, Rev. Sci. Instrum. **61**, 965 (1990).
[36]D. B. Mitzi, L. W. Lombardo, A. Kapitulnik, S. S. Laderman, and R. D. Jacowitz, Phys. Rev. B **41**, 6564 (1990).
[37]W. C. Lee, J. H. Cho, and D. C. Johnston, Phys. Rev. B **43**, 457 (1991).
[38]M. Onellion, M. Tang, Y. Chang, G. Margaritondo, J. M. Tarascon, P. A. Morris, W. A. Bonner, and N. G. Stoffel, Phys. Rev. B **38**, 881 (1988); P. A. P. Lindberg, Z.-X. Shen, B. O. Wells, D. S. Dessau, D. B. Mitzi, I. Lindau, W. E. Spicer, and A. Kapitulnik, *ibid.* **39**, 2890 (1989).
[39]S. A. Elrod, A. Bryant, A. L. de Lozanne, S. Park, D. Smith, and C. F. Quate, IBM J. Res. Dev. **30**, 387 (1986).
[40]For example, P. K. Hansma and J. Tersoff, J. Appl. Phys. **61**, R1 (1987).
[41]Ch. Renner, Ph.D. thesis No. 2620, University of Geneva, Switzerland, 1993.
[42]C. K. Shih, R. M. Feenstra, and G. V. Chandrashekhar, Phys. Rev. B **43**, 7913 (1991).
[43]K. Yvon and M. François, Z. Phys. B **76**, 413 (1989), and references therein.
[44]S. A. Sunshine *et al.*, Phys. Rev. B **38**, 893 (1988).
[45]Y. Gao, P. Lee, P. Coppens, M. A. Subramanian, and A. W. Sleight, Science **241**, 954 (1988).
[46]H. L. Edwards J. T. Markert, and A. L. de Lozanne, Phys. Rev. Lett. **69**, 2967 (1992).
[47]D. S. Dessau, Stanford University (private communication); M. Onellion, University of Wisconsin (private communication).
[48]M. D. Kirk, C. B. Eom, B. Oh, S. R. Spielman, M. R. Beasley, A. Kapitulnik, T. H. Geballe, and C. F. Quate, Appl. Phys. Lett. **52**, 2071 (1988); C. K. Shih, R. M. Feenstra, J. R. Kirtley, and G. V. Chandrashekhar, Phys. Rev. B **40**, 2682 (1989).
[49]A. Yamamoto, M. Onoda, E. Takayama-Muromachi, F. Izumi, T. Ishigaki, and H. Asano, Phys. Rev. B **42**, 4228 (1990).
[50]H. Hancotte, D. N. Davydov, M. Ye, and R. Deltour, Physica B **204**, 206 (1995).
[51]T. Hasegawa, M. Nantoh, S. Heike, A. Takagi, M. Ogino, M. Kawasaki, H. Koinuma, and K. Kitazawa, J. Phys. Chem. Solids **54**, 1351 (1993).
[52]Ch. Renner and Ø. Fischer, Physica C **235-240**, 53 (1994).
[53]For example, H. Van Kempen, in *Scanning Tunneling Microscopy and Related Methods,* Vol. 184 of *NATO Advanced Study Institute, Series E: Applied Sciences,* edited by R. J. Behm *et al.* (Kluwer Academic, Dordrecht, 1990), p. 241.
[54]For example, K. Kadowaki, T. Mochiku, H. Takeya, Y. Saito, and K. Hirata (unpublished); P. Müller, Physica C **235-240**, 289 (1994).
[55]F. Sharifi, A. Pargellis, and R. C. Dynes, Phys. Rev. Lett. **67**, 509 (1991).
[56]Physica C **235-240**, 289 (1994).6 A. Kussmaul, J. G. Moodera,

G. M. Roesler, Jr., and P. M. Tedrow, Phys. Rev. B **41**, 842 (1990).

[57]T. Hasegawa, M. Nantoh, A. Takagi, H. Ikuta, M. Kawasaki, H. Koinuma, and K. Kitazawa, J. Phys. Chem. Solids **53**, 1643 (1992).

[58]M. D. Kirk, J. Nogami, A. A. Baski, D. B. Mitzi, A. Kapitulnik, T. H. Geballe, and C. F. Quate, Science **242**, 1673 (1988), and references therein.

[59]R. Escudero, E. Guarner, and F. Morales, Physica C **166**, 15 (1990).

[60]G. E. Blonder, M. Tinkham, and T. M. Klapwijk, Phys. Rev. B **25**, 4515 (1982).

[61]The spectra are measured using a digital-to-analogue output from the computer to generate the bias voltage, and an analogue-to-digital input to record the spectra. Thus taking fewer data points over a fixed energy range or increasing the lock-in time constant yields a lower energy resolution, with an experimental broadening of sharp features in the tunneling spectra.

[62]C. G. Olson, R. Liu, A.-B. Yang, D. W. Lynch, A. J. Arko, R. S. List, B. W. Veal, Y. C. Chang, P. Z. Jiang, and A. P. Paulikas, Science **245**, 731 (1989); D. S. Dessau, Z.-X. Shen, D. M. King, D. S. Marshall, L. W. Lombardo, P. H. Dickinson, A. G. Loeser, J. DiCarlo, C.- H. Park, A. Kapitulnik, and W. E. Spicer, Phys. Rev. Lett. **71**, 2781 (1993); Jian Ma, C. Quitmann, R. J. Kelley, P. Alméras, H. Berger, G. Margaritondo, and M. Onellion, Phys. Rev. B (to be published).

[63]D. S. Dessau, B. O. Wells, Z.-X. Shen, W. E. Spicer, A. J. Arko, R. S. List, D. B. Mitzi, and A. Kapitulnik, Phys. Rev. Lett. **66**, 2160 (1991); Y. Hwu, L. Lozzi, M. Marsi, S. La Rosa, M. Winokur, P. Davis, M. Onellion, H. Berger, F. Gozzo, F. Lévy, and G. Margaritondo, *ibid.* **67**, 2573 (1991).

[64]D. Mandrus, L. Forro, D. Koller, and L. Mihaly, Nature **351**, 460 (1991).

[65]However, note that this result does not rule out the possibility of a gap in the quasiparticle spectrum above T_c, which contribution would enhance the dip at zero bias due to the normal-state DOS.

[66]J. F. Zasadzinski, N. Tralshawala, P. Romano, Q. Huang, J. Chen, and K. E. Gray, J. Phys. Chem. Solids **53**, 1635 (1992).

[67]Several papers address the issue of the dip at about -70 meV in the DOS of BSCCO, though without talking about the asymmetry we observe in *c*-axis STM tunneling spectra. See, for example, Georgios Varelogiannis, Phys. Rev. B **51**, 1381 (1995), and references therein.

[68]J. E. Hirsch, Phys. Rev. B **50**, 3165 (1994).

[69]R. C. Dynes, V. Narayanamurti, and J. P. Garno, Phys. Rev. Lett. **41**, 1509 (1978).

[70]B. Barbiellini, Ø. Fischer, M. Peter, Ch. Renner, and M. Weger, Physica C **220**, 55 (1994).

[71]H. Won and K. Maki, Phys. Rev. B **49**, 1397 (1994).

[72]J. M. Byers, M. E. Flatté, and D. J. Scalapino, Phys. Rev. Lett. **71**, 3363 (1993); P. I. Soininen, C. Kallin, and A. J. Berlinski, Phys. Rev. B **50**, 13 883 (1994); N. Schopohl and K. Maki (unpublished).

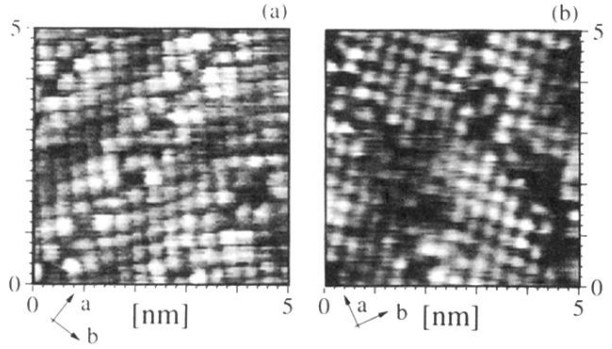

FIG. 1. Constant-current STM topographic images of *in situ* cleaved $Bi_2Sr_2CaCu_2O_{8+\delta}$ single crystals at 4.8 K (raw data). (a) Surface which shows a superconducting gap (imaging parameters: $I=275$ pA, $V_s=0.5$ V, $R=1.8$ GΩ). (b) Surface which shows a semiconducting gap ($I=300$ pA, $V_s=0.5$ V, $R=1.7$ GΩ).